Biomaterials 260 (2020) 120215

Contents lists available at ScienceDirect

Biomaterials

journal homepage: www.elsevier.com/locate/biomaterials

CaproGlu: Multifunctional tissue adhesive platform

Ivan Djordjevic [a,1], Oleksandr Pokholenko [a,1], Ankur Harish Shah [a,1], Gautama Wicaksono [a], Lluis Blancafort [b], John V. Hanna [c], Samuel J. Page [c], Himansu Sekhar Nanda [a,d], Chee Bing Ong [e], Sze Ryn Chung [f], Andrew Yuan Hui Chin [f], Duncan McGrouther [f], Muntasir Mannan Choudhury [f], Fang Li [f], Jonathan Shunming Teo [f,g], Lui Shiong Lee [f,g], Terry W. J. Steele [a,*]

[a] School of Materials Science and Engineering, Nanyang Technological University, 639798, Singapore
[b] Departamento de Química and Instituto de Química Computacional i Catálisis. Facultad de Ciències, Universidad de Girona, C/M.A. Capmany 69, 17003, Girona, Spain
[c] Department of Physics, University of Warwick, Gibbet Hill Rd., Coventry, CV4 7AL, United Kingdom
[d] Biomedical Engineering and Technology Laboratory, Department of Mechanical Engineering, PDPM-Indian Institute of Information Technology, Design and Manufacturing (IIITDM)-Jabalpur, Dumna Airport Road, Jabalpur, 482005, MP, India
[e] Histopathology/Advanced Molecular Pathology Lab, Institute of Molecular and Cell Biology (IMCB), Agency for Science, Technology and Research, 61 Biopolis Drive, Level 6 Proteos Building, 138673, Singapore
[f] Singapore General Hospital, Department of Hand Surgery, 169608, Singapore
[g] Sengkang General Hospital, Department of Urology, 544886, Singapore

ARTICLE INFO

Keywords:
Polycaprolactone
Bioadhesive
Diazirine
UVA
Diazoalkane

ABSTRACT

Driven by the clinical need for a strong tissue adhesive with elastomeric material properties, a departure from legacy crosslinking chemistries was sought as a multipurpose platform for tissue mending. A fresh approach to bonding wet substrates has yielded a synthetic biomaterial that overcomes the drawbacks of free-radical and nature-inspired bioadhesives. A food-grade liquid polycaprolactone grafted with carbene precursors yields CaproGlu. The first-of-its-kind low-viscosity prepolymer is VOC-free and requires no photoinitiators. Grafted diazirine end-groups form carbene diradicals upon low energy UVA (365 nm) activation that immediately crosslink tissue surfaces; no pre-heating or animal-derived components are required. The hydrophobic polymeric environment enables metastable functional groups not possible in formulations requiring solvents or water. Activated diazirine within CaproGlu is uniquely capable of crosslinking all amino acids, even on wet tissue substrates. CaproGlu undergoes rapid liquid-to-biorubber transition within seconds of UVA exposure–features not found in any other bioadhesive. The exceptional shelf stability of CaproGlu allows gamma sterilization with no change in material properties. CaproGlu wet adhesiveness is challenged against current unmet clinical needs: anastomosis of spliced blood vessels, anesthetic muscle patches, and human platelet-mediating coatings. The versatility of CaproGlu enables both organic and inorganic composites for future bioadhesive platforms.

1. Introduction

Each year millions of people undergo surgical procedures that require wound closure and tissue sealing. Mechanical fixation by suturing and stapling offers a cheap, reliable, and moderately fast method of addressing tissue fixation, but many drawbacks are known. Piercing fixation mechanisms carry the risk of nerve damage and entrapped tissue necrosis from injuries to the capillary vessels. The

* Corresponding author. Tel.: +65 6592 7594.
E-mail addresses: idjordjevic@ntu.edu.sg (I. Djordjevic), OPokholenko@ntu.edu.sg (O. Pokholenko), ANKUR006@e.ntu.edu.sg (A.H. Shah), GAUT0008@e.ntu.edu.sg (G. Wicaksono), lluis.blancafort@udg.edu (L. Blancafort), J.V.Hanna@warwick.ac.uk (J.V. Hanna), Sam.Page@warwick.ac.uk (S.J. Page), himansu@iiitdmj.ac.in (H.S. Nanda), cbong@imcb.a-star.edu.sg (C.B. Ong), szeryn.chung@mohh.com.sg (S.R. Chung), andrew.chin.y.h@singhealth.com.sg (A.Y.H. Chin), duncan.angus.mcgrouther@sgh.com.sg (D. McGrouther), muntasir.mannan.choudhury@singhealth.com.sg (M.M. Choudhury), fang.li@mohh.com.sg (F. Li), jonathan.teo.s.m@singhealth.com.sg (J.S. Teo), lee.lui.shiong@singhealth.com.sg (L.S. Lee), wjsteele@ntu.edu.sg (T.W.J. Steele).
[1] Equal Contributions, listed alphabetically.

https://doi.org/10.1016/j.biomaterials.2020.120215
Received 14 February 2020; Received in revised form 28 May 2020; Accepted 20 June 2020
Available online 11 July 2020

prolonged stress at suture and staple interfaces provokes tissue degeneration and potential immunological rejection. In order to avoid tissue damage by suturing, stapling, or other mechanical means, tissue adhesives offer a method for gentle fixation, free of tissue damage and unnecessary secondary surgeries [1]. These attributes are required for anastomosis of blood vessels and intestines, soft tissue repair, and expansion of minimally invasive surgeries (MIS) [2]. A total reliance on suturing within MIS has engineered elegant, but expensive robotics few clinics can afford [3–5]. A current unmet need exists for an on-demand tissue adhesive capable of suture strength fixation, rapid application, and cured material properties that mimic soft tissues.

Current commercial formulations are based on animal derived fibrin-thrombin proteins and cyanoacrylate synthetic polymers [1]. Fibrin-based glues are relatively weak in terms of adhesion strength, but are the only option for bonding internal tissues [6]. Cyanoacrylates are the gold standard in terms of instant adhesion strength, but formaldehyde and preservative leachates limit them to topical applications—internal use is contraindicated [1]. A range of free radical, click-chemistry, and bioadhesive mimics are under development [7–10], but these are based on translation of legacy thermosetting plastics or complex nature-based mechanisms (catechol and coacervates) requiring multicomponent initiators, inhibitors, and anaerobic environments. These are commercially, regulatory, and ethically challenging for clinical translation. Fresh approaches are required to combine the advantages of the aforementioned adhesives into one flexible platform incorporating rapid activation (less than 60 s), mimicking tissue elasticity (10–1000 kPa), and bonding of soft, wet substrates with no toxic initiators, preservatives, or byproducts. Development of an original tissue adhesive platform requires a reactive functional group that targets multiple amino acids (covalent bonding) paired with commercially available reputable biomaterials that offer resilience with a bioresorbable nature.

Towards the latter, few biomaterials have a better reputation than the family of polycaprolactone (PCL) materials. Caprolactone polyesters were introduced in the 1970s and PCL-based implants have followed with a wide spectrum of medical applications, including sutures, wound dressings and fixation devices [11]. A beneficial feature of PCL polyesters is the availability of branched, liquid oligomers that do not require solvents or plasticizers for low viscosity (less than 2 Pa.s) remedies. Branched oligomers (e.g. PCL-triol, PCLT) within the polyurethane industry has made them a readily available and inexpensive commodity (<10 USD/kg). Previous investigations of crosslinked PCLT/citric acid polymer was found to have compliant biomechanical elasticity to tissues [12]. The compliant nature of PCLT with its inherent hydrophobic environment provides an opportunity for activating metastable functional groups not possible in aqueous formulations. Metastable diazoalkane is a well-known reagent in organic syntheses to yield clean alkylations of carboxylic acids, among other nucleophiles. However, classic synthesis of this crosslinking group entails hazardous risks, preventing incorporation in biomaterials. In other words, it is too reactive to be handled safely. An isomer of diazoalkane, diazirine, is stable at room temperature and can be easily handled with little risk of side reactions. Light activation of diazirine produces transient carbene and diazoalkane—both ideal for bonding to protein backbones and multiple amino acids. Particularly stable is the family or trifluoromethylphenyl diazirine (TPD) molecules that maintain their stability even at temperatures up to 80 °C. These attributes are exploited for photoaffinity reagents to crosslink drug scaffolds to macromolecules [13–16]. Carbenes create new covalent bonds via insertion into X–H bonds (where X is C, N, O, S, etc)—a finding that can be employed to non-specifically crosslink any protein [17]. Undiscriminated crosslinking feature enables covalent grafting of TPD molecule onto polymer backbones resulting in bioadhesive formulations for polymer/tissue interfacial bonding.

Polyamidoamine (PAMAM) dendrimer-based adhesives have served as model systems for the development of voltage and UVA curable bioadhesive designs [18,19]. The structure activity relationships learned from these model systems is expanded to produce CaproGlu: a TPD-grafted food-grade PCLT that demonstrates exceptional biomaterial properties as a novel, UVA-active tissue adhesive. Diazirine end-groups on CaproGlu convert rapidly into metastable functional groups that covalently bond tissue surface proteins, thus providing strong interfacial adhesion (Fig. 1A). The major feature of CaproGlu is a film-forming polymer with liquid-to-biorubber crosslinking transition that provides biomechanically compliant tissue approximation. This novel adhesive has unique ability to adhere onto wet surfaces as a result of metastable intermediates that covalently anchor to the tissue substrate. Key attributes in choosing diazirine as a soft tissue crosslinking group include benign derivatives (evolution of molecular nitrogen), initiator and preservative free, stabile under ambient light conditions, and a range of activation methods, including handheld UVA LEDs, low-voltage currents, ultrasound, and thermal activation [19–24]. Diazirine-grafted PCLT (liquid CaproGlu) activates at low dose of UVA light of 10–20 J cm^{-2}, which is 5–10 times lower than average daily dose received by sunlight [25]. CaproGlu is a unique acrylate-free formulation that covalently inserts into wet tissue proteins through carbene insertion [17].

CaproGlu allows fine tuning by three parameters: (1) ratio of grafted diazirine; (2) UVA dose; and (3) concentration/type of solid organic/inorganic fillers that provide either hygroscopic characteristics for interfacial adhesion on wet tissue surfaces (citric acid; CA), enable strong support for hard bone tissue (hydroxyapatite; HA) and prevention of thrombogenesis (sebacic acid; SA) by anionic surface segments [26]. In addition, tricarboxylic CA and dicarboxylic SA are anticipated to increase crosslinking kinetics with the metastable diazoalkanes, further improving mechanical moduli and adhesion strength. CaproGlu's hydrophobic, liquid material properties are further exploited for controlled release of hydrophobic drugs for localized drug delivery. Various formulations of CaproGlu are investigated for the structure – adhesive performance properties with *ex vivo* and *in vivo* experimental models. In order to assess translation into medical devices, the formulation is gamma-sterilized with the recommended radiation dose (25 kGy) [27]. Sterilized samples are subsequently tested for any alteration in chemical structure, mechanical modulus and adhesion strength. *In vivo* investigation is divided into 3 parts: (1) subcutaneous implantation-rat model for preliminary assessment of potential foreign body reaction (inflammation and giant cell formation); (2) bupivacaine local drug delivery model from crosslinked CaproGlu/drug composites, and (3) surgical anastomosis supported by UVA-crosslinked CaproGlu. Tissues with CaproGlu films are dissected and examined for evidence of chronic inflammation, thrombosis, fibrosis and other pathological changes. For the first time, CaproGlu's UVA curing into an elastomeric biorubber and bonding of various soft tissues is evaluated against unmet clinical applications. CaproGlu's potential as a multipurpose tissue adhesive platform is demonstrated together with tunable human platelet response, as well as biocomposite formation with both organic and inorganic solid compounds.

2. Materials and methods

2.1. CaproGlu synthesis and characterization

Polycaprolactone triol (CAPA 3031, 300 Da, Perstorp, Sweden) and diazirine-bromide (TCI, Japan) are mixed in PCLT/diazirine molar ratios of 1/1 and 1/2 to yield 50% and 70% of diazirine conjugation respectively (referred to as CaproGlu PCLT-D50 or PCLT-D70). Reactants are dissolved in dioxane and allowed to react in the presence of silver oxide (Ag_2O) and molecular sieve for 72 h at room temperature under nitrogen atmosphere. Filtered product is precipitated in deionized water and centrifuged; the water-dioxane supernatant is discarded and the PCLT-D conjugate product (viscous pale-yellow transparent liquid) is further washed 3 times with water and centrifuged. PCLT-D formulations are lyophilized for 24 h and characterized with ^{1}H NMR to calculate the

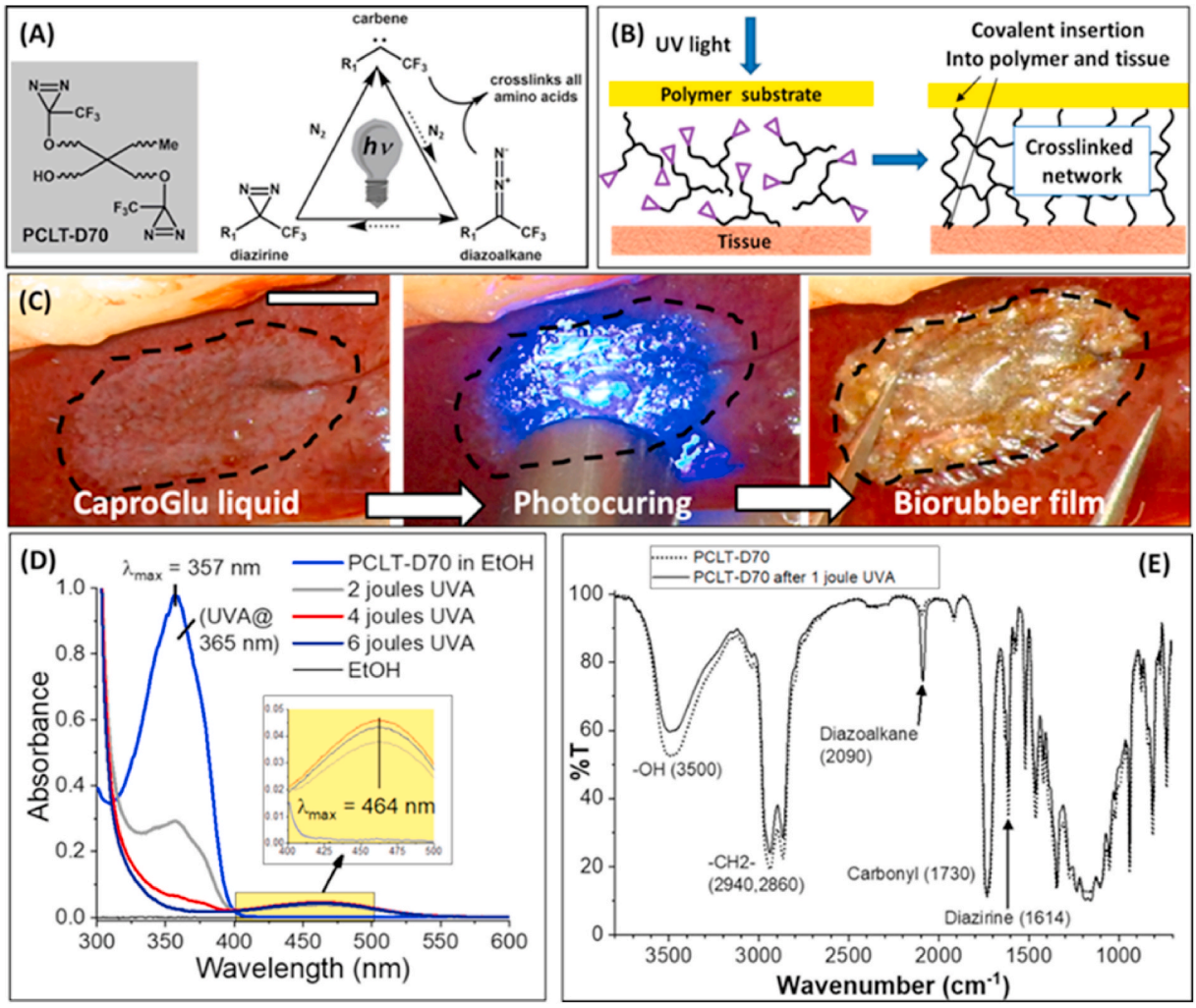

Fig. 1. CaproGlu Tissue Adhesive Platform. (**A**) CaproGlu is synthesized by grafting PCLT –OH endgroups with diazirine UVA-active group (R_1 = phenyl bromide). Adhesive crosslinking is initiated by UVA light (365 nm) that converts diazirine into reactive groups of carbene (half-life in ns to ms) and diazoalkane (half-life sec to hours); dashed arrows represent minor pathways rarely observed. (**B**) Demonstration of sandwich substrate cross-linking between transparent polymer and tissue as well as intermolecular crosslinking. (**C**) Video 1 stills of liquid-to-elastomeric transition of CaproGlu (PCLT-D70 mixed with citric acid at 10% w/w) upon UVA activation on hydrated surface of rabbit liver and adhesion demonstration by pull test with tweezers (scale bar = 5 mm). (**D**) UVA curing kinetics of diluted CaproGlu–decrease of diazirine peak intensity at 357 nm and appearance of diazo peak at 464 nm upon curing; diazirine $t_{1/2} = 5 \pm 1$ s @ 200 mW cm^{-2} or ED50 = 0.9 ± 0.2 J. (**E**) FTIR spectra of raw and cured PCLT-D70 recorded after exposure to 1J of UVA light.

conjugation (grafting) percentage (Bruker Avance; 400 MHz). The adhesive curing kinetics upon increased UVA dose is recorded with ^{19}F NMR: the depletion of diazirine peak and appearance of newly formed diazo and ether bonds are determined quantitatively over the increase in curing UVA energy up to 25 J. FTIR spectroscopy is used in ATR mode to record spectra of PCLT-D before and after low energy curing (1 J) to detect and confirm the presence of diazo peaks. UVA-induced depletion of diazirine peak at 365 nm is monitored with UV spectroscopy. Composite formulations are prepared by mixing PCLT-D70 with the following solid components: citric acid (CA; 10% w/w), hydroxyapatite (HA; 50% w/w) nanopowder (particle size < 200 nm) and sebacic acid (SA; 10%, 20% and 30% w/w) by mixing with spatula. Mechanical properties (dynamic modulus and adhesion strength) are determined for all CaproGlu formulations by photorheometry and lap shear adhesion test (experimental details and design are in Supplementary Information).

2.2. Animal studies

All experiments are performed with the approval of the Institutional Animal Care and Use Committee (IACUC). Subcutaneous *in vivo* implants are evaluated on Wistar rats: subcutaneous implantation (IACUC #: ARF-SBS/NIE-A0301). Bupivacaine loaded CaproGlu is implanted in Sprague-Dawley male rats: localized delivery (IACUC #: 2016/SHS/1186). *In vivo* implants are evaluated on rabbits: iliac artery anastomosis after full-moon (FM) and half-moon (HM) splice compared to conventional interrupted suturing (control), CaproGlu + polymer mesh and neat CaproGlu. 10-week old Wistar female rats (300 ± 50 g) are purchased from InVivos Pte Ltd (Singapore). Animals are sedated with inhalation of isoflurane (2%) and the analgesic is administered by intraperitoneal (IP) injection (tramadol, 3 mg/kg). New Zealand white rabbits are purchased from Bio Conquest Pte Ltd (Singapore). Rabbits weighing between 2 kg and 4 kg are randomly selected irrespective of age or gender. These animals received care in compliance with the guidelines from IACUC #: 2016/SHS/1213, and approval from Singapore General Hospital's ethics committee. Interrupted suturing employed Ethilon 10/0 sutures with the aid of 25× microscopic magnification. All rabbits are anaesthetized with intramuscular Ketamine (35–50 mg/kg) and Xylazine Hydrochloride (5–10 mg/kg), with maintenance on inhalational Sevoflurane throughout the surgery. Intravenous Enrofloxacin is given for antibiotic prophylaxis according to the rabbits' weight, in addition to intravenous crystalloids for fluid

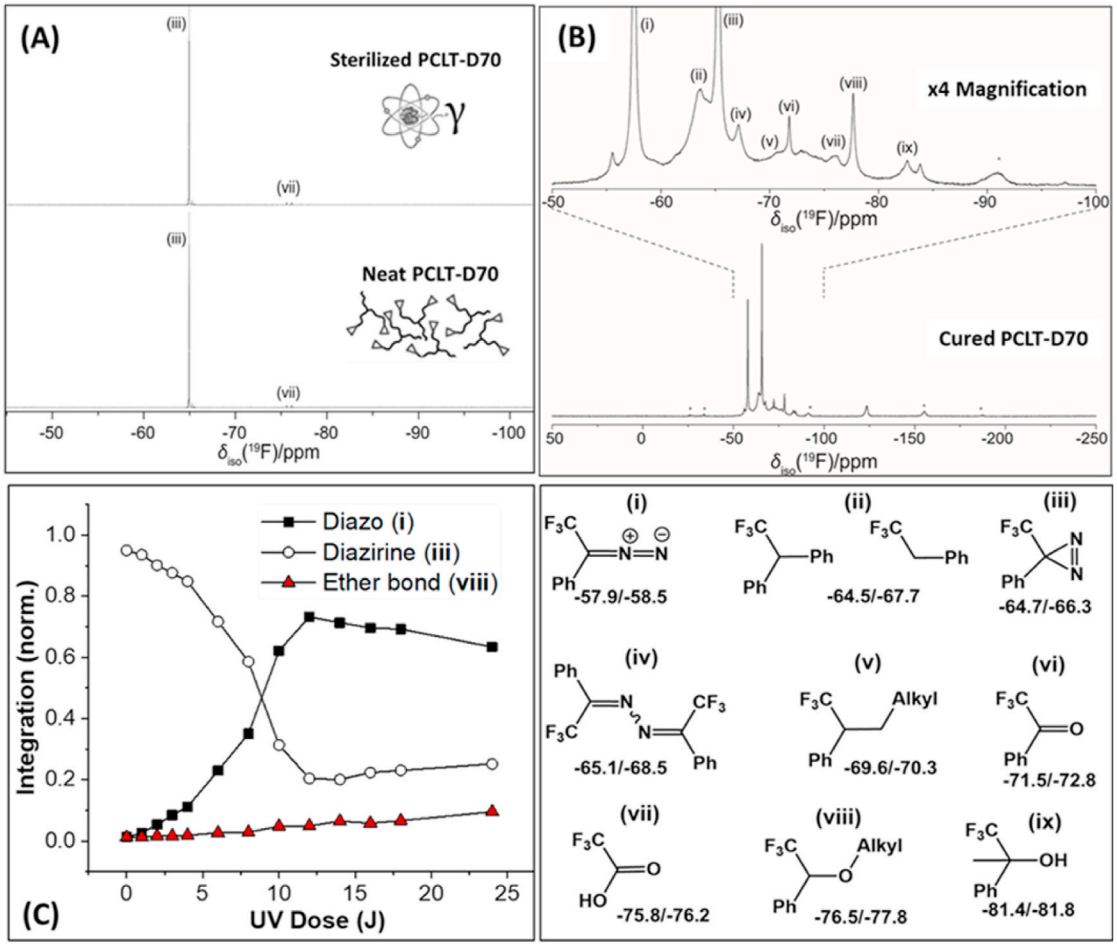

Fig. 2. The effect of UVA curing and gamma-sterilization on diazirine structure measured with ^{19}F NMR. (A) Recorded spectrum of raw (uncured) CaproGlu (PCLT-D70; bottom) and spectrum of gamma-sterilized raw PCLT-D70 (top) - peak (iii) is characteristic for diazirine and shift (vii) originates from trifluoro acetate. (B) Magnified spectrum recorded in solid state of PCLT-D70 after UVA curing with 25 J dose; (i – ix) peak assignment, chemical shifts and corresponding structures. (C) Curing kinetics: depletion of diazirine (iii) on the account of metastable diazoalkane isomer (i) and covalent intermolecular crosslinking by carbene insertion into –C–O–H forming ether bonds (–C–O–Alkyl; vii).

maintenance during surgery. Continuous monitoring of heart rate and rhythm, blood pressure, as well as oxygen saturation is performed throughout the surgery. *Ex vivo* tissues are procured for lap shear adhesion tests: bovine muscle tissue (Prime Supermarket, Singapore), porcine aorta (Primary Industry Abattoir, Singapore) and porcine cranial bone slides (2 cm × 4 cm x 0.5 cm Singapore General Hospital). Crosslinking of CaproGlu is performed with Convoy S2+ 365 nm Nichia UV LED Flashlight with the power of 100 mW cm^2 at the distance from the site of 2 cm; the absorbed UVA dose is not higher than 10 J (equivalent to 100 s of UVA irradiation).

2.3. Subcutaneous implantation: full thickness wound model

Subcutaneous implantation is performed as preliminary study in order to determine the immunological response to CaproGlu prior to anastomosis experiments. Skin is shaved and surgical area is sterilized with povidone iodine solution followed by 70% ethanol. Four full-thickness wounds (1.5 cm long/0.5 cm deep) are made on the dorsum of each rat exposing the muscle tissue. Liquid CaproGlu (PCLT-D70) formulation is first applied by spatula onto PLGA patches (diameter = 6 mm; thickness = 0.1 mm) and implanted directly on exposed muscle tissue (PLGA patches without bioadhesive are used as control). Bioadhesive patches are crosslinked with UV light from approximately 2 cm distance (~100 mW cm^{-2} for 1 min: 6 J cm^{-2}). Once the sample is fixed, the wound is closed with Maxon™ 3-0 sutures. Animals are monitored and the body weight is recorded during the course of 7 days. On the 7th day, the animals are sacrificed and the dissected samples of skin with epidermal and dermal suture implants as well as internal implant material are fixed in formalin prior to histology analysis.

2.4. In vivo local drug delivery from crosslinked adhesive

Interaction of CaproGlu (PCLT-D50) adhesive with local anesthetic (Bupivacine HCL) with muscle tissue is performed by implanting and photocuring the adhesive onto the gastrocnemius (calf) muscle subcutaneously. On the day of experiment (day 0), each animal is allowed to run through a 1-m box and the runs are recorded prior to surgical implantation. Each rat is then sedated with isoflurane (2%) and the analgesic is administered by intraperitoneal (IP) injection (tramadol, 3 mg/kg). On each rat, two full-thickness wounds are made (1.5 cm long/0.2 cm deep) through the dermis and facia to expose the gastrocnemius muscle of the hind limbs. CaproGlu (50 mg) with and without bupivacaine is applied by pipette directly on exposed muscle tissue and photocured with UVA dose of 10 J. The surgical incision is closed with VicrylTM 3-0 sutures (polyglactin) through the facia with a subsequent postoperative dose of antibiotic. In the course of 7 days, the animals are monitored for mobility, box speed and body weight. On the 7th day, the animals are sacrificed and the implant site including the skin, epidermal, dermal and muscle tissue is dissected and fixed in formalin for blind histological analysis.

2.5. Anastomosis of small diameter iliac artery: rabbit model

The total of 15 rabbits were procured for the animal studies exploiting the iliac bifurcation with dual anastomosis sites at the left common iliac artery (CIA-L) and right common iliac artery (CIA-R). Out of 15 rabbits, 12 survived the anastomosis experiments. Due to complications during surgery 2 animals died; 1 animal died post-implantation: a subsequent autopsy revealed thrombosis in both iliac arteries. Both CIA-L and CIA-R are first either partially spliced (half-moon; HM) or fully spliced (full-moon; FM) followed by anastomosis of the CIAs by one of the following three methods: 1) suture control with eight continuous interrupted sutures (n = 7); 2) Four-suture anastomosis reinforced with 3D-printed polycaprolactone mesh (PCL, Perstop, M_w = 50 kDa; printed with Janome desktop robot JR2000NE; pore size 1 mm × 0.5 mm) fixed with UVA-activated CaproGlu (n = 8); and 3) eight-suture anastomosis reinforced with UVA-activated CaproGlu (no mesh; n = 5). Methods 2) and 3) utilize CaproGlu PCLT-D70. Dose-adjusted intravenous Lidocaine is given prior to clamping of the first vessel. For Method 1), a double microvascular clamp is placed onto CIA, and the artery is spliced between the clamps with straight micro scissors perpendicular to the long axis of the vessels. Both the proximal and distal ends of the vessel lumen are dilated via a micro-dilator. Adequate trimming of the adventitia and irrigation of the proximal and distal vessel ends with heparinized saline is performed. Method 2) employed four stiches (placed at 90° apart), which is reinforced using a PCL mesh fixed onto iliac surgical site by UVA crosslinking of CaproGlu. PCL mesh is square cut four times the circumference of the blood vessel to wrap the vessel twice. A primer layer (5% w/v CaproGlu solution in anhydrous absolute ethanol) is brushed on the tissue and UVA activated for 15 s. The PCL mesh is wrapped on anterior side of vessel wall and CaproGlu is brushed on, followed by UVA irradiation for 60 s (irradiated twice for 30 s with an interval of 30 s between the irradiation window with total dose of 10 J). The double clamps are removed after 60–120 s. Anastomosis time is charted. If bleeding was observed after clamp removal, a moistened gauze with light pressure stopped the blood leakage. Once the clamp is released, uninterrupted blood flow without leakage is observed. The anastomosis is judged to be completed if there is no leak after 2 min. Method 3) completely spliced CIA is anastomosed with 8 simple interrupted sutures and reinforced with UV cured CaproGlu (UVA dose = 10 J). The three Methods required ten rabbits which were closely monitored postoperatively and are kept in isolation for 7 days. Two additional rabbits were anastomosed via Method 3) on both CIA-L and CIA-R and observed for 21 days for long-term recovery and visual postmortem traces of CaproGlu on surgical site (n = 4). On postoperative day 7 or day 21, vessel patency is assessed again under general anesthesia and the anastomosis sites of both CIA-L and CIA-R (Method 1–3; 10 animals@7 day; total of 20 dissected artery samples and Method 3, 2 animals@21 day; total of 4 dissected artery samples) are then harvested for histopathological evaluation.

2.6. Histopathology analysis

Histopathology of all implant samples is performed by board-certified pathologist. For subcutaneous implants, the tissue is sectioned perpendicular to the skin surface and parallel to plane of incision. For rabbits (anastomosis) the surgical site is reopened and both iliac arteries are harvested. The extracted/harvested tissues are placed into cassettes and processed with Sakura VIP Tissue Processor, through increasing alcohol concentrations and finally with xylene and paraffin. After processing, tissues are embedded into paraffin block and sectioned with rotary microtome into 5 μm thick sections: perpendicular section to skin surface for rats and a longitudinal section for the anastomosed CIA's in rabbits. The slides with tissue/sample sections are dried and placed into incubator (60 °C/15 min) before haemotoxylin and eosin (H&E) staining with Leica Autostainer XL. Subsequent 5 μm thick sections are prepared and stained by Masson Trichrome (MT) histochemical stain to confirm collagen extraction. All the MT slides are digitized with Ariol SL-50/Leica SCN400 slide scanner (Leica Microsystems, Germany). Images are scanned at 20x, exported to Slidepath Digital Image Hub (Leica Microsystems, Germany) for viewing, and analyzed using Ariol software/Slidepath TissueIA software (Leica Microsystems, Germany).

2.7. Statistics

One-way ANOVA statistical analysis was performed by Tukey's comparison and $P < 0.05$ was set as significant in all the tests. Data are presented as mean values ± standard deviation. All the calculations and graphs were produced in OriginPro software.

3. Results

3.1. Motivation of CaproGlu tissue adhesives

Tissue adhesives have many (often opposing) design parameters that must be met for a clinically applicable solution. They need to be tissue reactive (but non-toxic), flexible (with tough adhesion), and instantly activated (yet shelf-stable). Key considerations in the CaproGlu platform is overcoming weak adhesion to wet substrates with a *synthetic methodology*. Towards the latter, inexpensive resorbable oligomers that are liquid under ambient conditions confine the list to a few polyols, including hydrophobic PCLT and branched polyethylene glycol (PEG). The latter observes unfavorable aqueous swelling properties—PCLT's aqueous insolubility avoids this liability. Of the available food-grade PCLTs, the 300 Da variant (CAPA 3031) is chosen for its relatively high hydroxyl density and low viscosity (560 mg KOH/g and η = 0.17 Pa.s @ 24 °C, respectively). Diazirine serves as the precursor crosslinking agent (Fig. 1A; Fig. S1), due to its known formation of reactive groups after UVA (340–390 nm) exposure. Several variants of diazirine exist, but these are restricted to commercially available diazirine structures that allow rapid grafting onto PCLT triol in a one-step scalable methodology. UVA-induced diazirine ring degradation results in generation of molecular nitrogen, either directly from diazirine or indirectly through semi-stable diazoalkane. In terms of diazirine-grafted polymer adhesives, generation of molecular nitrogen yields a porous structure that may aid in rapid bioresorption [19]. The two compositions of PCLT-D (50% and 70% grafting) serve different purposes. PCLT-D50 aims to be soft and compliant for local drug release with no appreciable load bearing. PCLT-D70 has a higher dynamic modulus and adhesion strength for load bearing applications, such as tissue approximation in anastomosis repairs.

3.2. CaproGlu demonstration on liver with diazoalkane detection after UVA exposure

Aryl-diazirine displays conversion kinetics ten times faster than alkyl-diazirine (Fig. S1B), with the former predicted by CASPT2/CASSCF theory to form metastable diazoalkanes (Fig. S2)—hence aryl-diazirine (referred to as diazirine in subsequent text) is the only variant considered henceforth. Diazirine is grafted to PCLT (Fig. 1A; Fig. S1) in predetermined ratios to yield the CaproGlu platform via the Williamson ether synthesis (Fig. S3). After purification, the *neat* CaproGlu is transparent, pale-yellow liquid with an oil-like consistency. Low UVA exposure transitions the formulation from a low viscosity liquid, into an indiscriminate crosslinked adhesive that can form interfacial covalent bonds on both polymers and tissues as well as intermolecular crosslinking (Fig. 1B; Fig. S1A). CaproGlu PCLT-D70 with hygroscopic citric acid (CA) applied to liver tissue adheres to the wet liver substrates as observed in Video 1 and video stills in Fig. 1C. Adhesion and reaction kinetics are hypothesized to be enhanced with CA, where a composite is formulated by mixing it directly with CaproGlu (10% w/w). After activation, an adhesive biorubber foam remains. A wide range of material properties is possible through simple alterations in UVA dose, diazirine

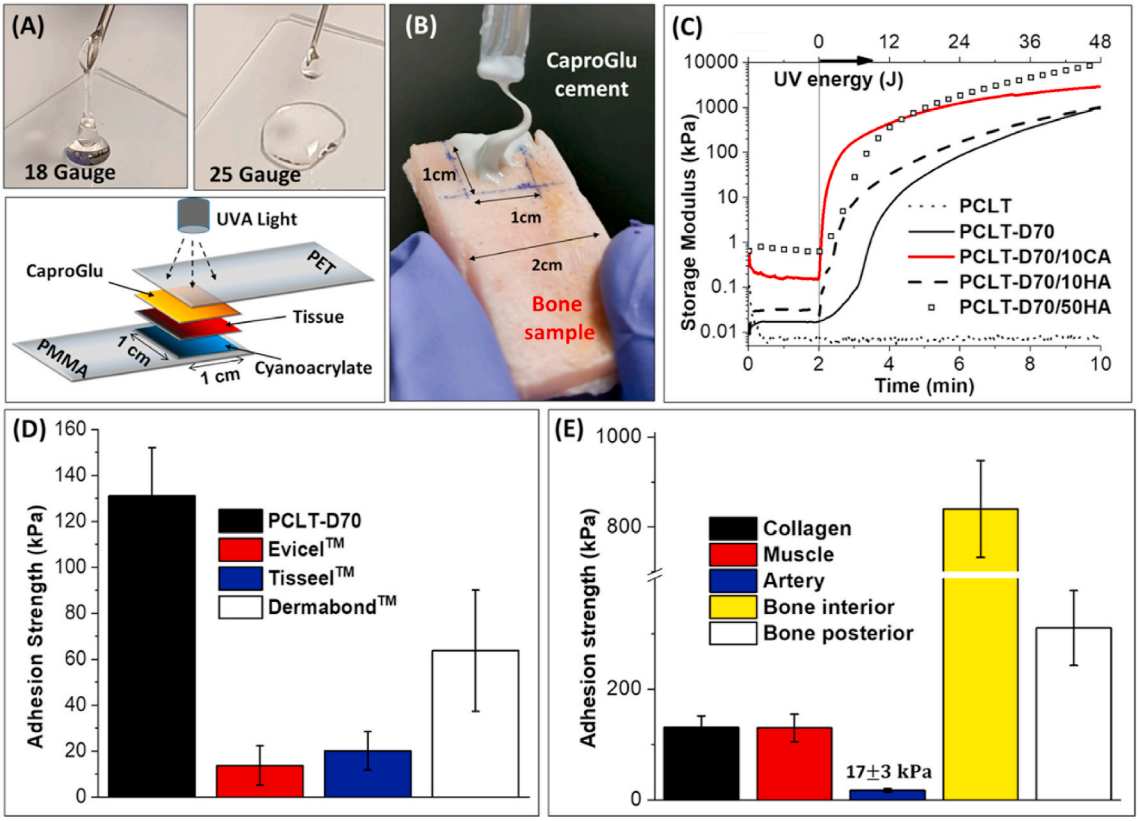

Fig. 3. Adhesion strength and elasticity of CaproGlu. (A) CaproGlu liquid formulation through 18 (0.85 mm ID) and 25 (0.26 mm ID) gauge needles (top). Experimental design of lap-shear adhesive strength–tissue fixation onto PMMA slide, application of CaproGlu and subsequent UVA-activated crosslinking (bottom). (B) Photograph of liquid CaproGlu/hydroxyapatite (HA) composite on cranial bone sample prepared for lap shear adhesion test. (C) Dynamic mechanical moduli measured with photorheometry - comparison of neat CaproGlu (PCLT-D70) with ungrafted PCLT (control). Composites include citric acid (10%, w/w; PCLT-D70/10CA) and hydroxyapatite (10%, 50% w/w HA for PCLT-D70/10HA and PCLT-D70/50HA respectively). (D) Shear adhesion strength of CaproGlu PCLT-D70 and commercial tissue sealants on hydrated collagen substrates; (E) Lap shear adhesion strength for PCLT-D70 on different tissue substrates; muscle tissue formulation, PCLT-D70/10CA and bone tissue formulation, PCLT-D70/50HA. Each adhesion test has minimum of four replicates.

grafting percentage (CaproGlu PCLT-D50 and PCLT-D70), and/or incorporation of solid additives. UVA doses of 1–2 J (10–20 s exposure); display rapid activation of diluted CaproGlu (in ethanol, Fig. 1D). The diazirine halflife ($t_{1/2}$) under these diluted conditions is 5 ± 1 s (at 200 mW cm^{-2}) and UVA effective dose (ED) to reach 50% of the starting concentration is 0.9 ± 0.2 J (Fig. 1D). Quantum yield of diazirine grafted CaproGlu calculates to 2.5% from 2 J UVA exposure. This is within the range of 1–13% reported by others [28]. FTIR spectra of *neat* CaproGlu (Fig. 1E) shows formation of the metastable intermediate diazoalkane (peak at 2090 cm^{-1}, Fig. 1E) after low UVA energy dose of 1 J. This diazoalkane is a semi-stable intermediate that selectively crosslinks acids (i.e. CA or SA) and other nucleophiles [29]. If no nucleophiles are present, diazo peak remains persistent in FTIR even after 30 min post UVA activation (for detailed interpretation of FTIR spectra and quantitative determination of diazo decay kinetics see Supplementary Information; Fig. S4).

Supplementary video related to this article can be found at https://doi.org/10.1016/j.biomaterials.2020.120215

Carbene's transient picosecond half-life prevents direct detection under ambient conditions [30]. Diazoalkane displays extraordinary stability and UVA-dose dependent formation within the hydrophobic PCLT environment. Crosslinking characterization is aided by diazirine's $–CF_3$ group, which serves as a molecular tag for ^{19}F NMR analysis (Fig. 2). As an example, Fig. 2A displays the ^{19}F NMR spectra of CaproGlu before and after gamma sterilization (25 kGy dose). The spectra yields no perturbation of grafted diazirine group or effect on CaproGlu function; (see Supplementary Information for mechanical properties before and after gamma sterilization). Equally important is the absence of potentially toxic species such as HF (−198 ppm [31]) and fluoroform (CHF_3, -79.5 ppm [32]) in recorded spectra of *neat* UVA-activated CaproGlu in Fig. 2B. Analysis of crosslinked CaproGlu via ^{19}F solid-state NMR in Fig. 2B yields multiple broad spectra, indicative of several crosslinking mechanisms by the metastable functional groups of carbene and diazoalkane (see Table S1; Fig. S5). A cumulative UVA dose analysis tracks the growth of diazoalkane, ether crosslinks (via carbene insertion onto free –OH groups of PCLT), and consumption of diazirine in Fig. 2C. Diazirine decay from neat CaproGlu of 50% is reached at ED50 of 7 ± 3 J. After 10–12 J, the relative concentration of diazoalkane intermediate peaks and decays thereafter, presumably to more carbene intermediates. Diazirine is known to yield diazomethane/carbene in ratios of 35/65 [33]. Previous reports indicate 20–35% conversion of diazirine into linear diazoalkane with a half-life ranging from 18 s to 22 min, where the interplay is shown in Fig. 1A and Fig. S1A [34,35].

3.3. CaproGlu bonds wet tissues and is impervious to gamma sterilization

CaproGlu's liquid properties allow *neat* or composite formulations for a wide array of applications. The low viscosity ($\eta^* < 2$ Pa.s, similar to pancake syrup) of *neat* CaproGlu is easily metered with narrow bore syringe needles, as applied to solid substrates for lap shear adhesion tests in Fig. 3A. Rheological profiles for PCLT-D50 and PCLT-D70 are shown in Fig. S6. It should be noted that the original viscosity of PCLT is 0.17 Pa.s. High solid content mixtures of PCLT-D70/HA (HA 10% and 50%, w/w) yields a spreadable paste, as pictured in Fig. 3B. Photo-rheometry is a powerful method to evaluate the liquid to solid viscoelastic properties in real-time or as a function of UVA dose. Fig. 3C displays the

range of formulations under UVA exposure of 0–60 J cm^{-2}. *Neat* PCLT observes no change in elasticity—no crosslinking is observed without diazirine grafting. PCLT-D70 formulation crosslinks rapidly after 2 min of UV activation and storage moduli (G′) values reached 30 kPa. The crosslinking reaction continues at slower rate and G′ reaches relatively stable value of 900 kPa after 8 min post UVA (Fig. 3C). The loss modulus (G″) is also measured and gelation point (G' = G″) is reached at UVA activation dose of 1.8 J (Fig. S6). The amplitude sweep profile of CaproGlu (PCLT-D70 at 1 Hz) is recorded immediately after 20 J of UVA showing elastomeric behavior as the crosslinked adhesive allows 100% strain before yield (Fig. S6). According to the International Commission on Non-Ionizing Radiation Protection (ICNIRIP) the recommended safe dose for UVA (365 nm) should not exceed 27 J cm^{-2} [36]. In order to comply with those regulations all the experiments in this paper are referenced to the UVA energy dose (J). CaproGlu reached G' > 100 kPa upon the absorption of 10 J and that dose is selected for all *in vivo* experiments.

Unlike PCLT-D70, PCLT-D50 reached maximum G' value of 10 kPa and gelation point after 2 J of UVA dose (Fig. S6). PCLT-D50 was only used for localized drug delivery (*in vivo*) and not for load bearing applications. A range of tunable shear moduli from 1 to 10,000 kPa measured for PCLT-D70 and composites is evident. This opens the possibility of mimicking moduli of organs/muscle (10–100 kPa), tendons/ligaments (100–1000 kPa) and bone tissues (>10 MPa) [37–39]. CaproGlu (PCLT-D70) benchmarked to commercial tissue adhesives observes a stronger lap shear bond on wetted collagen substrates in Fig. 3D. CA is a hygroscopic component that enables interfacial crosslinking through surface water interactions. Fig. 3E summarizes CaproGlu and corresponding composites on hard and soft tissue substrates. The shear adhesion strength of 17 kPa to wet artery tissue meets the requirement for sealing artificial defects as other hydrophobic sealants have observed [7]. The experimental set-up for adhesion on both hard and soft tissues is shown in Fig. S7. HA/CaproGlu composite observes higher adhesion strength on bone interior compared to bone exterior, which may be due to surface roughness (Fig. S8 graphs the stress vs strain displacement curves in Fig. 3D and E).

Since UVA-generated carbene from CaproGlu macromolecular endgroups covalently inserts in both polymer and tissue surfaces, the adhesive failure is cohesive as shown in Fig. S7; Adhesive strengths of 20–800 kPa are observed, depending on the substrate and formulation under evaluation. CaproGlu composites with CA or HA increase adhesion strength and shear modulus, with the speculated mechanism arising from the solid additives' hygroscopic and toughening agent attributes [40–43]. The chemistry of CaproGlu remains consistent after a gamma sterilization dose of 25 kGy [27], with the adhesive function maintained (Fig. S9).

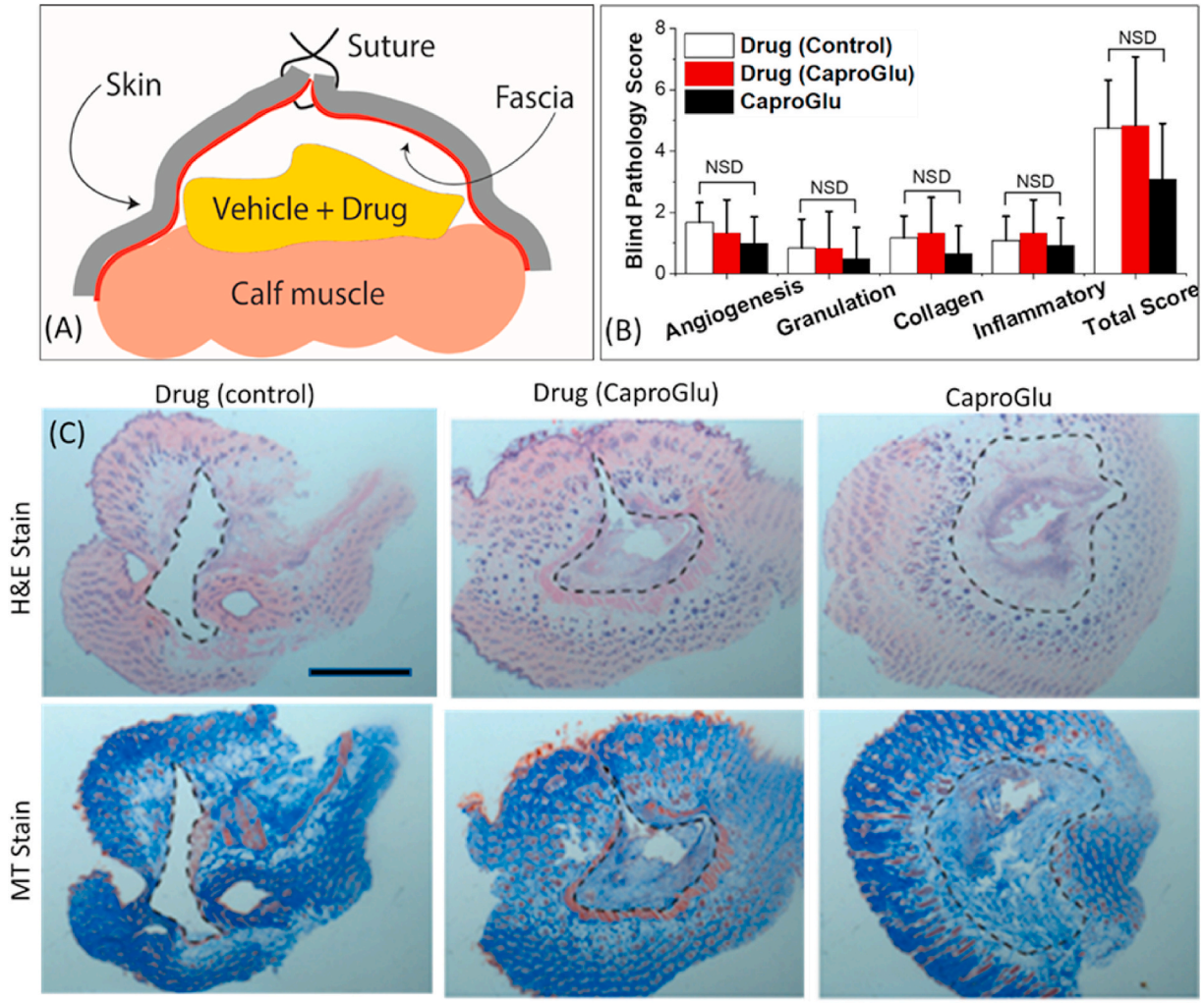

Fig. 4. CaproGlu anesthetic drug delivery vehicle. (A) Schematic of the subcutaneous implant onto the calf (gastrocnemius) muscle of 10-weeks old Sprague-Daley male rats. Full procedures are shown in Video 2 (CaproGlu implant) and Video 3 (mobility evaluation). (B) Pathology evaluation of extracted muscle from sacrificed animals after 7 days post-implantation (n = 5; NSD = no statistical difference, *p < 0.05). (C) Histological examination by H&E and Masson's trichrome (MT) stains (size bar = 5 mm). Localy injected drug (control; left), CaproGlu loaded with drug (middle) and pure CaproGlu.

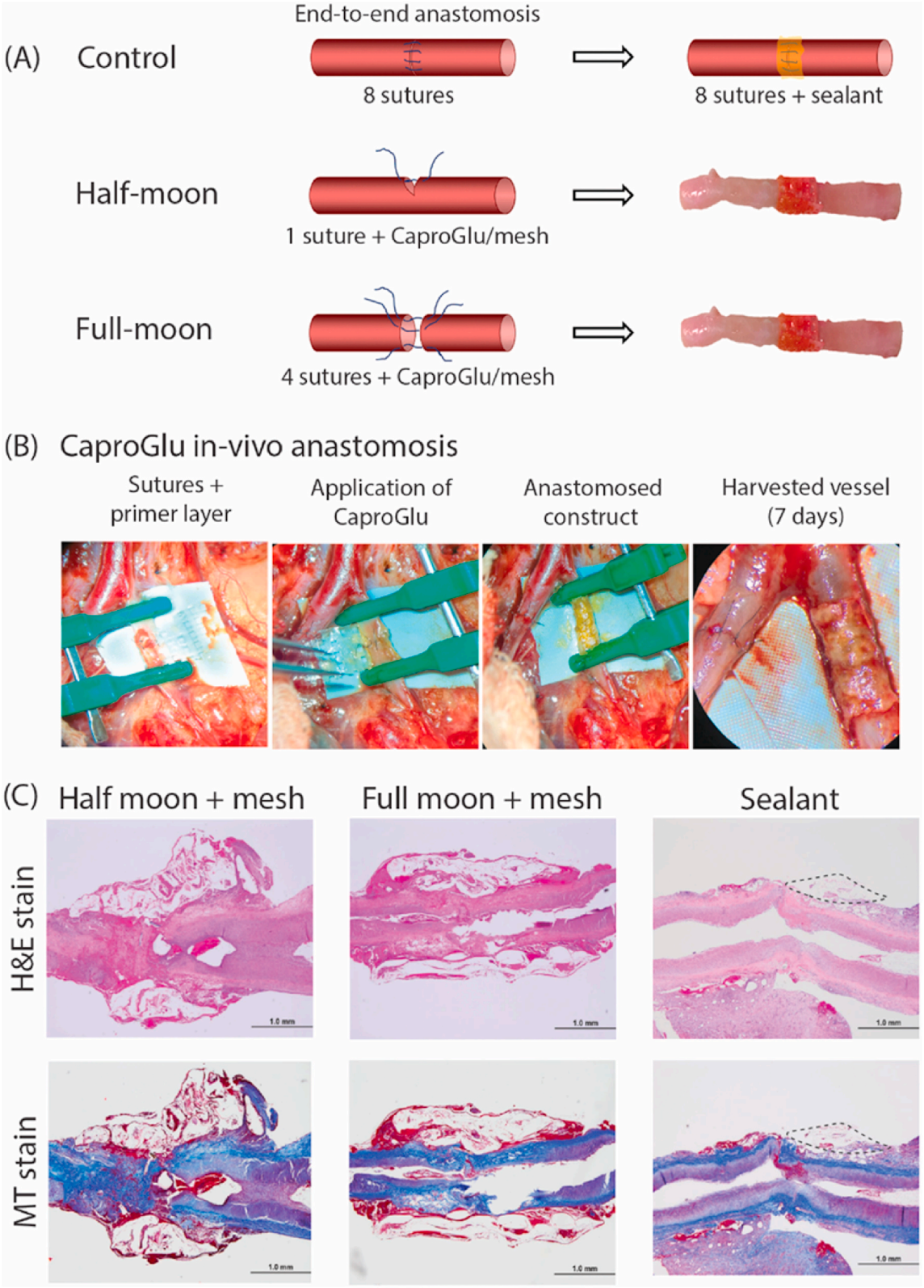

Fig. 5. Rabbit artery anastomosis. (A) Schematic of vascular repair through continuous interrupted sutures (control, 7 day). Extended 7 (n = 4) & 21 day (n = 4) implants are performed with application of CaproGlu as sealant. Half-moon and full-moon anastomosis is aided with PCL mesh. (B) Sequence of artery anastomosis: Application of primer layer (5% CaproGlu) followed by mesh fixation with UVA activation of CaproGlu. The iliac anastomosis is complete after a 4π wrap and the ligatures removed. After one week, the vessel is harvested for prepared for histological evaluation. (C) H&E and Masson's Trichrome (MT) stained images of the repaired illiac artery (cross-sections are not midline) from the left: half-moon (partially spliced) and full-moon anastomosis (on the surface of the artery remains the CaproGlu/mesh that is infiltrated with soft tissues). Continuous interupted sutures with neat CaproGlu as sealant–dash line marks the CaproGlu sealant implant. Size bar = 1 mm.

3.4. Unmet clinical challenge: fixation of rapidly resorbed anesthetic films

Locally injected anesthetics such as bupivacaine are indispensable for avoiding the side effects of general anesthesia. However, these drugs have a rapid clearance rate where local anesthesia is limited to a few hours. CaproGlu's unique material properties offer a novel solution to extend local anesthesia up to a few days as the liquid polymer can readily dissolve bupivacaine (logP = 3.6) within the hydrophobic matrix. As a precaution before larger animal trials, subcutaneous implants are first compared between CaproGlu and medical grade polyesters (PLGA; Fig. S10A-C). PLGA results in a thicker fibrous capsule, but both had similar upregulation of macrophage cells. Overall, they have similar histological profiles (Fig. S10D-G), clearing the way for the 3-arm non-inferiority challenge of CaproGlu/bupivacaine composites. Upon activation, the CaproGlu/bupivacaine composite is glued to the rodent calf muscle within a full thickness wound, with subsequent evaluation of rodent mobility (see Video 2; Video 3 and Fig.S11A). Bupivacaine is hypothesized to diffuse into the pores, eventually reaching sink conditions (50 mg kg^{-1}), where dynamic movements stimulate the delivery of the anesthetic from elastomeric carrier [44]. CaproGlu's tunable viscoelasticity is exploited to give a low shear modulus (~10 kPa @ 20J UVA, tan delta = 1.35; for PCLT-D50 used only in drug delivery experiments Fig. S6) that readily yields with normal tissue dynamics, but doesn't flow out of the wound site (e.g, Bingham plastic). The 3-arm non-inferiority challenge is evaluated with: 1) drug (control); 2) drug (CaproGlu); and 3) *neat* CaproGlu. The injected drug (control) is the standard treatment of 0.5% bupivacaine in saline. The drug (CaproGlu) arm consists of CaproGlu (PCLT-D50) loaded with 10% bupivacaine (9:1 wt ratio). The subcutaneous implantation and the results are demonstrated in Fig. 4. All three arms are applied on a full thickness wound, directly on a rodent calf muscle as shown in Fig. 4A and Fig. S11. The initial burst release of a 50 mg drug (CaproGlu) implant has a similar dose as a 0.25 mL bolus of 0.5% bupivacaine in saline (1.2–1.6 mg; Fig. S11). After day 7 the rodents are sacrificed and histology specimens evaluated blindly by certified pathologist. Scored biocompatibility markers in Fig. 4B display that drug (CaproGlu) and *neat* CaproGlu are non-inferior to drug (saline). In terms of rodent mobility, only the drug (CaproGlu) formulation had an improvement in walking speed, but there was no statistical improvement versus the Drug (Control) under similar time point (Fig. S11). Overall, CaproGlu drug release vehicle displays non-inferiority in comparison to locally administered drug by injection. Histological evaluations of the full thickness wound observe that the majority of the CaproGlu is resorbed and replaced with vascularized collagen tissue as seen in Fig. 4C. Masson Trichrome (MT) staining observes fibrous capsule present in drug (CaproGlu), but not in the *neat* CaproGlu or drug (control) as indicated with dash line.

Supplementary video related to this article can be found at https://doi.org/10.1016/j.biomaterials.2020.120215

3.5. Unmet clinical challenge: blood vessel anastomosis and suture sealant

Arterial anastomosis is a procedure to join blood vessels across tissue transplants—a procedure that requires considerable training by experienced surgeons. End-to-end anastomosis employs sutures to align opposed blood vessels, as seen in Fig. 5A. Overall, the procedure is technically complicated, time consuming, and limited to blood vessels greater than 1 mm. Methods to reduce or remove sutures would decrease surgical time and target smaller blood vessels. To assess CaproGlu PCLT-D70 for this procedure, our team took a de-risked stepwise approach: 1) optimization on *ex vivo* arteries, 2) repair of a half-moon spliced iliac artery, then a full-moon end-to-end anastomosis. *Ex vivo* anastomosis (in Fig. 5A) of 3–5 mm swine carotid arteries provided a model system for trial and error approaches. By incorporating a 3D printed PCL mesh within CaproGlu (Fig. S12), reliable anastomosis seals could withstand hydrostatic burst pressures of 108 ± 16 mmHg as measured on *ex vivo* porcine model (the modified ASTM F2392-04 methodology is described

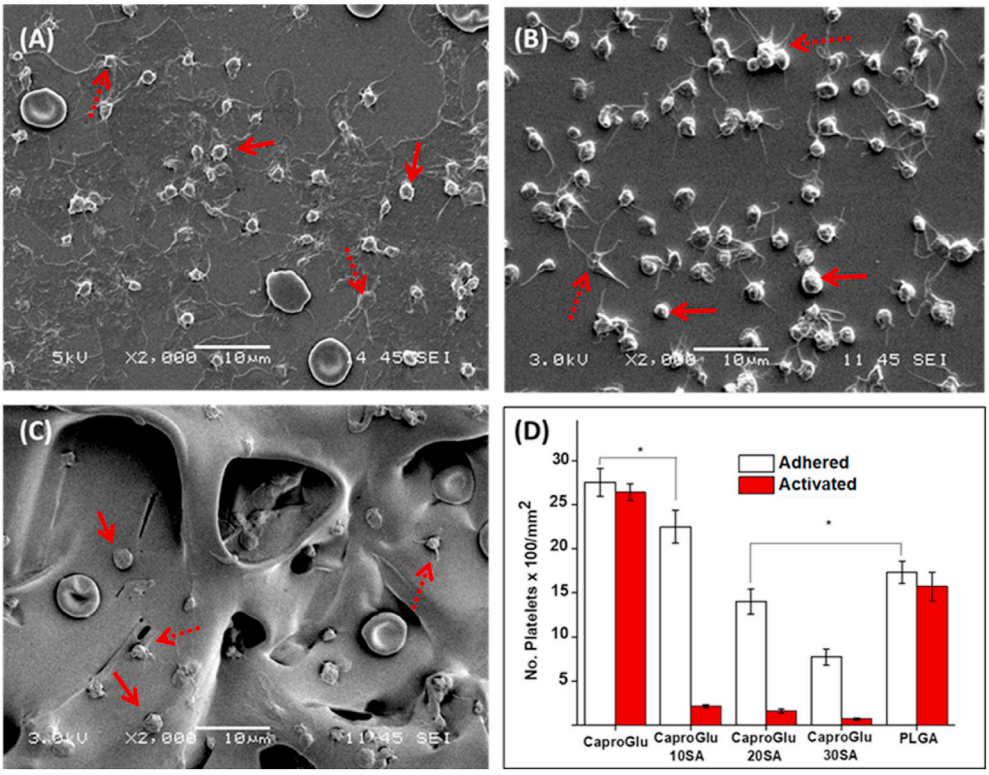

Fig. 6. Human derived platelet rich plasma (PRP) exposure of CaproGlu surface coatings. Scanning electron microscopy of PRP exposed (A) PLGA (control), (B) neat CaproGlu and (C) composite CaproGlu/30SA (30% sebacic acid w/w). Solid arrows: adhered platelets in inactivated/resting stage. Dashed arrows: adhered, activated platelets with pseudopodia. (D) Adhered and activated platelets (per mm^2) counted from SEM images (*significant differnce = $p < 0.05$).

in Supplementary Information). CaproGlu sealed blood vessel sustains the burst pressure higher than control (4 sutures; no adhesive; 52 ± 4 mmHg).

The optimized *ex vivo* approach is translated to rabbit iliac arteries, where the 8-suture anastomosis (control) and the CaproGlu composites/PCL mesh are applied to both (left and right) iliac arteries (Fig. S12). The stepwise procedure given in Fig. 5B provides the general approach for half-moon and full-moon operations. A primer layer of CaproGlu is brushed on, UVA cured, and covered with a CaproGlu/PCL mesh 4π wrap (200% of circumference, Video 4). Anastomosis is complete after UVA exposure and ligatures removed (Video 5). Blood leakage is minimal and occlusion through the wrap is complete in 2–3 min. After seven days, infiltration of soft tissues is apparent and the CaproGlu/PCL mesh has expanded with the pulsing iliac artery (Video 6); representative histology evaluations are given in Fig. 5C. Inflammation and fibrosis within the implant locality ranged from mild to moderate, with no statistical difference from sutured anastomoses (representative pathologist histological descriptions and comparative pathological scores are in Fig. S13). *Neat* CaproGlu could be exploited as a sealant for sutures, as seen in the 7 day implant of Fig. 5C. After 21 day post-surgery, neat CaproGlu sealant was completely absorbed, as polymer remnants are not observed after vessel extraction nor detected in histological examination.

Supplementary video related to this article can be found at https://doi.org/10.1016/j.biomaterials.2020.120215

3.6. Unmet clinical challenge: tissue adhesives with tunable platelet adhesion/activation

Similar to other biomaterials, tissue adhesives in immediate contact with blood will evoke fibrinogen adsorption and may lead to platelet activation [45,46]. Secreted proteins from adhered platelets enhance platelet-platelet interaction and lead to the formation of fused platelet plugs. Accelerating or preventing the biochemical interactions is required for hemostasis (e.g. tumor occlusion) or endovascular implants (e.g. resorbable stents), respectively. Platelet morphological changes give a direct assessment of platelet activation [47] (activated and adhered platelets on biomaterials surface; Fig. 6). Negatively charged hydrophobic additives (such as SA) are hypothesized to decrease platelet adhesion, platelet activation, or both due to electrostatic surface repulsion [48,49]. CaproGlu/SA 10–30 (PCLT-D50 with 10%. 20% and 30% SA, w/w) composites challenge this hypothesis by direct observation of human blood on the composite surface. After curing, exposure of the composite coatings to platelet rich plasma (from healthy human volunteers) elicits quantitative platelet adhesion and activation.

Two types of platelet morphology are identified according to previously published protocol on diazirine-grafted PAMAM dendrimer bioadhesive (PLGA control, Fig. 6A) [50]. CaproGlu (Fig. 6B), and SA/CaproGlu composite (Fig. 6C). Inactivated platelets have a spherical morphology (solid arrow); activated platelets display multiple pseudopodia (dashed arrow). The ratio of both are summarized in Fig. 6D (SEM images in Fig. S14) where the platelet adhesion and activation decrease with addition of solid SA composite component. Reduction of platelet adhesion and activation supports the electrostatic surface repulsion hypothesis. Addition of 10% SA decreased activation by an order of magnitude. Higher ratios decreased the number of adhered platelets. SA is biochemically metabolized as other fatty acids, serves as a common plasticizer, and typically derived from castor oil—a renewable resource. Attempts to evaluate CaproGlu/10% SA composites on full moon anastomosis (as described above) were abandoned after blood clotting time was found to be greater than 5 min.

4. Discussion

The CaproGlu platform is motivated by the unmet clinical need of versatile tissue adhesives. Many are attempting new bioadhesives, but few are focusing on improvements in chemical crosslinking strategies. The current trend of tissue adhesives relies on ill-suited plastic polymerization techniques (e.g. free radical, urethane) or complex nature mimicking events (e.g. catechols, coacervation). Neither of these strategies allow covalent bonding to multiple amino acids present on tissue surfaces. CaproGlu sets itself apart by exploiting reactive intermediates known to crosslink all amino acids, which has been exploited for photoaffinity protein labeling [51]. Photoaffinity investigations generally report non-selective carbene insertion, but with some preference towards nucleophilic functional groups. Selectivity depends on many factors, including local environments, substituents, and carbene/diazoalkane ratios [52]. The preclinical results described herein attempt to exemplify the platform's exclusive bonding chemistry where no current adhesives are applicable, e.g. *in situ* implants, vascular repair, and platelet mediating films. The CaproGlu/bupivacaine composite demonstrates a simple strategy for forming *in situ* implants free of organic solvents with a relatively low injectable viscosity. *In situ* bupivacaine implants with 3 days of local anesthesia have the promise of reducing post-operative opiate use, improving recovery time, and shortening the duration of hospital stays [53,54]. However, current designs require solvent plasticizers (e.g. benzyl alcohol) that can cause unwanted local irritations and hypersensitivity reactions [54,55]. CaproGlu's water-free formulation is speculated to be more stable than collagen-derived implants and provide better fixation than aqueous liposomal formulations [56,57].

CaproGlu's fixation ability is also exploited for vascular repairs, which would be suitable for minimally invasive surgeries. Vascular anastomosis has the primary objective of establishing blood flow between host and replanted tissues—it is essential in many clinical specialties encompassing trauma, transplants, and plastic surgery. Despite the importance of this operation, the suturing techniques remain principally unchanged since the first developments by Dr. Alexis Carrelin in 1906, which earned him the Nobel prize in 1912. Advancements that could reduce or remove the number of sutures are fundamental for anastomoses of small blood vessels (<1 mm) and translation to minimally invasive surgeries. To the best of our knowledge, the CaproGlu mesh composite is the first bioresorbable adhesive that allows a reduction of sutures without incorporating balloon catheters. The tissue adhesive had similar histological outcomes compared to an interrupted suture anastomosis. Our earlier anastomosis investigations evaluated intima apposition techniques with cyanoacrylate tissue sealants, but these had a high degree of inflammation and fibrosis resulting in acellular zones [58]. In contrast, the CaproGlu mesh composite displayed healthy tissue infiltration with no acellular zones after one week. Sealant implants of neat PCLT-D70 with shear moduli of ~100 kPa were resorbed within 3 weeks (in rabbits, n = 4) compared to one week of PCLT-D50 (in rats, n = 5). In contrast, photocured poly (glycerol sebacate acrylate; PGSA)-based vascular sealants [7] take longer than one year to fully resorb [59]. Previous studies have investigated the swelling properties of thermally crosslinked polycaprolactone triol (the same precursor used to produce CaproGlu) with citric acid. Crosslinked elastomer swells in the range of 8–20% (water) depending on the crosslinking density [12]. Similar range is expected for CaproGlu with tunable mechanical modulus.

Human-derived platelet rich plasma (PRP) incubation on cured CaproGlu surfaces gives a facile method of assessing the thrombotic potential. The platelet activation results demonstrate that *neat* CaproGlu has a mild activation similar to PLGA polyesters, where red blood cells remained intact. Inclusion of sebacic acid reduced platelet activation by a factor of 10, but was not fully arrested. CaproGlu/sebacic acid composites anastomosis trials had to be abandoned due to increased time needed for blood clotting. This suggests that the CaproGlu anastomosis results may partly rely on its hemostatic properties. The CaproGlu platform relies on reactive intermediates that can crosslink all amino acids, but the tradeoff is the limited density of covalent networks. The generation of nitrogen will limit the matrix density—preventing stiff

material properties typical of acrylates and epoxies—however such stiffness is elective, and foams may have better compliance for mimicking anisotropic tissues. In addition, elastomeric porous scaffolds observe cellular migration and moderation of foreign body response in comparison to solid implants. Immunological response is known to be dependent on pore-size and free-radicals [60]. CaproGlu's dissipation of free radicals (as judged by benign effects of gamma sterilization) supports an inherent antioxidant activity, which is beneficial for wound healing applications [61].

The benefits of a one-step synthesis between diazirine and PCLT has the promise of straightforward GMP scale-up for commercialization and regulatory submissions—issues that limit many nature-mimicking bioadhesives. While low molar mass diazomethanes and some chlorodiazirines need to be treated with caution, the trifluoro-diazirine exhibits no observable unstable behavior, even under high heat conditions they have an endothermic decomposition above 90 °C. Food-grade PCLT is a readily available commodity and diazirine synthesis is straightforward from available ketone scaffolds. The generation and arrest of reactive intermediates (diazoalkane) from photo-activated diazirine is only possible through the hydrophobic environment created by the PCLT grafting as demonstrated by UV absorption, FTIR, and ^{19}F NMR. Diazoalkanes cleanly crosslink nucleophiles such as carboxylic acids, amines, hydroxyls, and thiols [62–65]. The extended stability of diazoalkane intermediate in the PCLT matrix was not expected, but may be exploited for double-sided tissue adhesion or alternatives for high-strength pressure sensitive adhesives. With respect to the stable diazoalkanes, carboxylate-containing powders (citric acid, sebacic acid) were incorporated into the matrix, which resulted in several advantages: an increase in crosslinking kinetics, rapid gelation time (<30 s), and higher elastic moduli. The improvements result from the rapid alkylation of carboxylic acids by the diazoalkane intermediate. Apart from their role as a composite fillers, solid hygroscopic organic acids (i.e. citric acid) have multiple attributes including temporal dehydration of tissue surfaces, inhibition of competing hydrolysis reactions [66], and pH-induced bactericidal properties [67].

PCLT belongs to the platform of PCL-based biomaterials that are known for their relatively slow degradation kinetics and stability in both acidic (pH = 1) and alkaline (pH = 13) environments up to 3 days at physiological temperature [68]. Furthermore, degradation of PCL-based polymers can range up to many years [11]. PCL undergoes ester hydrolysis and the degradation products are eliminated through fatty acid and citric acid metabolic pathways [69]. Although we have not performed systematic study of biodegradation, CaproGlu is expected to undergo the same, well-established degradation pattern for PCL-based crosslinked materials. The versatility of PCL-based biomaterials is well documented and that includes tissue adhesives [70–74]. The majority of these adhesives are based on PCL grafted acrylates. However, these and other liquid polyester acrylates have had little success in clinical translation. Experience has shown that acrylated biomacromolecules have a long list of detractors: 1) short-shelf lives despite refrigeration; 2) year-long bioresorption; 3) requires multiple leachable additives (initiators and free radical stabilizers); 4) necessitates preheating before application [75]; 5) relies on relatively weak mechanical interlocking for adhesion; and 6) inability to be gamma-sterilized [71]. This limits acrylate designs to niche applications, such as light activated sealants [59]. In contrast, CaproGlu is: 1) room temperature stable for 6 months; 2) resorbable in weeks; 3) initiator-free; 4) low viscosity/no preheating required; 5) adheres surfaces through strong covalent bonding; and 6) impervious to gamma-irradiation doses.

Gamma-irradiation sterilizes biomacromolecules through induction of free-radicals and is the method most commonly used to sterilize implantable medical devices, standardized to industrial scale. However, not all biomacromolecules can sustain gamma irradiation. In terms of proteins (i.e. Evicel™ or Tisseel™ commercial tissue sealants) gamma irradiation induces the oxidation of tryptophan and methionine residues along with isomerization of aspartic acid residues even at relatively low radiation dose 0.5–5 kGy (in comparison to 25 kGy recommended for medical devices) [76]. Acrylates (i.e. MeTro [77] or PGSA [7]) readily crosslink under gamma rays, converting from liquid to hard solid plastic. Similar to acrylates, succinimide oligomers are known to polymerize by gamma irradiation, although under much higher dose of 50 kGy [78]. Structural alteration of epoxy systems upon gamma exposure is also known to cause physical changes in the material [79]. Unlike other crosslinking macromolecules used as tissue sealants, our voltage-activated, electrocuring adhesives have shown that diazirine is 1 e^- reduced to a reversible diazirinyl radical [80,81], which likely accounts for its exceptional stability to free-radicals. Any gamma-induced electrons are dissipated over the semi-conductive diazirine network in contrast to induction of free radical polymerization in acrylate-grafted macromolecules. While PCL has been observed to be susceptible to gamma irradiation [82], this is only applicable to high molecular weight variants—CAPA 3031 (300 Da) within CaproGlu remains unaffected. Furthermore, CaproGlu has a clear advantage over existing commercial bioadhesives, such as the single component (no additives/initiators) formulation that crosslinks with all amino acids (diazirine is known for this feature from photoaffinity protein labeling procedures). Important features and advantages of CaproGlu over other tissue sealants are displayed in Table 1.

Several limitations within our results should be noted. The observations and preclinical trial conclusions are based on short term implants of one week in relatively small groups ($n \leq 8$) to reach the stated conclusions. Long term implants are required to evaluate extended biocompatibility considerations. Diazoalkanes have a mutagenesis risk and requires CaproGlu to be further evaluated by Ames mutagenesis assays which is one of the major objectives of our future work. Incorporation of therapeutics like bupivacaine crosslink to the adhesive matrix due to carbene insertion, and the percentage of retained/released drug has not been quantitatively investigated. Our future work will focus on these weaknesses and continue to expand liquid/moldable formulations, including exploration of CaproGlu thermal stability towards further viscosity modulation and incorporation as a 3D printing ink. The CaproGlu platform may be further expanded towards pressure

Table 1
CE approved tissue adhesives vs CaproGlu.

	Tisseal/Duraseal	Bioglue/ArterX	Dermabond/Histocryl	Setalium/MeTro	CaproGlu
Crosslinking Chemistry	Fibrin & thrombin	Albumin & aldehyde[a]	Cyano- acrylates	Methacrylate biopolymer	Carbene + PCLTriol
End-User Activation?				✓	✓
Activation time <1 min?			✓	✓[b]	✓
Adhesive >20 kPa?		✓	✓	✓	✓
Internal Use?	✓	✓		✓	✓
Pure Synthetic?			*V*[b]	✓ (Setalium)[b]	✓
Single Component?					✓
Crosslinks all amino acids?					✓
Gamma Sterilization?					✓

[a] Some formulations employ glutaraldehyde, others polyaldehyde.
[b] Requires free radical initiators and/or free radical stabilizers. Both are considered leachable and potentially allergenic.

sensitive tapes, strain-activated drug delivery systems, double side adhesion, and ^{19}F MRI contrast agents [83].

5. Conclusion

CaproGlu is a novel platform of tissue adhesives that allows rapid bonding of hydrated tissues in a liquid formulation free of any solvents. The unique crosslinking chemistry gives an unprecedented degree of control over adhesion strength and elasticity on a variety of tissue substrates. This formulation was validated on preclinical models of current unmet clinical needs, including strain-activated analgesia, vascular anastomosis, and modulation of human platelet interactions. CaproGlu's unique attributes of low viscosity and hydrophobicity make the tissue adhesive suitable for syringe application on irregular tissue surfaces. CaproGlu composites produced by simple mixing with powdered additives increases reaction kinetics, adhesion strength, and elasticity. Tuning of liquid to biorubber material properties is achieved by simple variation of three parameters: 1) ratio of grafted diazirine; 2) UVA dose; and 3) choice of powdered additive (e.g. citric acid, hydroxyapatite, and sebacic acid). The latter parameters extend the surgical applications. Hygroscopic citric acid reduces carbene fouling, speculated to remove water on tissue surface for direct interactions on organ surfaces. Hydroxyapatite nanoparticles induced strong tissue adhesion and elasticity suitable for bone repair. Sebacic acid reduces platelet activation in human blood through negatively charged electrostatic repulsion. These combined attributes of the CaproGlu platform demonstrates its multifunctional biomaterial roles for tissue approximation, wound healing, and sustained local delivery of therapeutic agents. The synthetic nature, simple one-step synthesis, and resistance to gamma-sterilization doses provides a pathway for future collaborations.

6. Significance statement

CaproGlu surgical adhesive rapidly transitions from a liquid prepolymer to a biorubber that adheres to wet tissues via carbene insertion chemistry—the unique crosslinking mechanism displays exceptional stability to gamma sterilization and long-term shelf storage under ambient conditions. To demonstrate the wet tissue bonding, CaproGlu is challenged against current unmet clinical needs, including mending of blood vessels, anesthetic muscle patches, and blood compatible coatings.

CRediT authorship contribution statement

Ivan Djordjevic: Conceptualization, Data curation, Formal analysis, Investigation, Methodology, Project administration, Writing - original draft, Writing - review & editing. **Oleksandr Pokholenko:** Data curation, Formal analysis, Investigation, Methodology, Project administration, Writing - original draft, Writing - review & editing. **Ankur Harish Shah:** Data curation, Formal analysis, Investigation, Methodology, Project administration, Writing - original draft. **Gautama Wicaksono:** Data curation, Formal analysis, Investigation, Methodology. **Lluis Blancafort:** Formal analysis, Investigation, Methodology, Funding acquisition. **John V. Hanna:** Formal analysis, Investigation, Methodology, Writing - original draft. **Samuel J. Page:** Formal analysis, Investigation, Methodology, Writing - original draft. **Himansu Sekhar Nanda:** Data curation, Formal analysis, Investigation, Methodology. **Chee Bing Ong:** Formal analysis, Investigation, Methodology, Writing - original draft. **Sze Ryn Chung:** Formal analysis, Investigation, Methodology, Writing - original draft. **Andrew Yuan Hui Chin:** Formal analysis, Investigation, Methodology, Writing - original draft. **Duncan McGrouther:** Formal analysis, Investigation, Methodology, Writing - original draft. **Muntasir Mannan Choudhury:** Formal analysis, Investigation, Methodology. **Fang Li:** Formal analysis, Investigation, Methodology. **Jonathan Shunming Teo:** Formal analysis, Investigation, Methodology, Writing - original draft. **Lui Shiong Lee:** Formal analysis, Investigation, Methodology, Writing - original draft. **Terry W.J. Steele:** Conceptualization, Formal analysis, Funding acquisition, Methodology, Project administration, Resources, Supervision, Validation, Visualization, Writing - original draft, Writing - review & editing.

Declaration of competing interest

Terry W.J. Steele and Ivan Djordjevic are co-inventors of patent application: Hygroscopic, Crosslinking Coatings and Bioadhesives; PCT/SG2018/050452. Authors declare no competing interests.

Acknowledgements

We thank the Singapore General Hospital, NTU-College of Engineering and the School of Materials Science & Engineering.

Appendix A. Supplementary data

Supplementary data to this article can be found online at https://doi.org/10.1016/j.biomaterials.2020.120215.

Funding

NTU-Surgery ACP, Strategic Joint Research Fund (SJRF): Fast, 2 min surgical procedure for splicing of blood vessels; Singapore General Hospital Research Grant (SRGOF16Jan29): Dynamic release of local anaesthetics through novel tissue adhesives; Ministry of Education Tier 1 Grant: Coil Expanding Layers (COELS) For Intravascular Repairs; Ministry of Education Tier 2 Grant: Tailored soft-tissue bioadhesives for site-specific therapy (MOE2012-T2-2-046) & CaproGlu, Double sided wet-tissue adhesives (MOE2018-T2-2-114); NTU-Northwestern Institute for Nanomedicine Grant: 3D-Printing of Electro-Curing Nanocomposite Living Electrodes for Cardiac Tissue Regeneration; NTUitive POC (Gap) Fund Aesthetic Applications of CaproGlu Bioadhesives NGF/2018/05/; A*Star IAF PP Grant (H19/01/a0/0II9): CathoGlu Bioadhesives-preventing catheter extravasation and skin infections. JVH acknowledges support for the solid state NMR instrumentation at Warwick used in this research which was funded by EPSRC (grants EP/M028186/1 and EP/K024418/1) the University of Warwick, and the Birmingham Science City AM1 and AM2 projects which were supported by Advantage West Midlands (AWM) and the European Regional Development Fund (ERDF).

Data and materials availability

All materials are commercially available or can be synthesized based on the methods.

References

[1] P.J.M. Bouten, M. Zonjee, J. Bender, S.T.K. Yauw, H. van Goor, J.C.M. van Hest, R. Hoogenboom, The chemistry of tissue adhesive materials, Prog. Polym. Sci. 39 (7) (2014) 1375–1405.
[2] C. Esposito, R. Damiano, A. Settimi, M. De Marco, P. Maglio, A. Centonze, Experience with the use of tissue adhesives in pediatric endoscopic surgery, Surg. Endosc. Other Intervent. Tech. 18 (2) (2004) 290–292.
[3] T. Leal Ghezzi, O. Campos Corleta, 30 Years of robotic surgery, World J. Surg. 40 (10) (2016) 2550–2557.
[4] A. Tan, H. Ashrafian, A.J. Scott, S.E. Mason, L. Harling, T. Athanasiou, A. Darzi, Robotic surgery: disruptive innovation or unfulfilled promise? A systematic review and meta-analysis of the first 30 years, Surg. Endosc. 30 (10) (2016) 4330–4352.
[5] A. Abiri, O. Paydar, A. Tao, M. LaRocca, K. Liu, B. Genovese, R. Candler, W. S. Grundfest, E.P. Dutson, Tensile strength and failure load of sutures for robotic surgery, Surg. Endosc. 31 (8) (2017) 3258–3270.
[6] I. Strehin, Z. Nahas, K. Arora, T. Nguyen, J. Elisseeff, A versatile pH sensitive chondroitin sulfate–PEG tissue adhesive and hydrogel, Biomaterials 31 (10) (2010) 2788–2797.
[7] N. Lang, M.J. Pereira, Y. Lee, I. Friehs, N.V. Vasilyev, E.N. Feins, K. Ablasser, E. D. O'Cearbhaill, C. Xu, A. Fabozzo, R. Padera, S. Wasserman, F. Freudenthal, L. S. Ferreira, R. Langer, J.M. Karp, P.J. del Nido, A blood-resistant surgical glue for

minimally invasive repair of vessels and heart defects, Sci. Transl. Med. 6 (218) (2014) 218ra6.
[8] B.D. Fairbanks, M.P. Schwartz, C.N. Bowman, K.S. Anseth, Photoinitiated polymerization of PEG-diacrylate with lithium phenyl-2,4,6-trimethylbenzoylphosphinate: polymerization rate and cytocompatibility, Biomaterials 30 (35) (2009) 6702–6707.
[9] M. Mehdizadeh, J. Yang, Design strategies and applications of tissue bioadhesives, Macromol. Biosci. 13 (3) (2013) 271–288.
[10] H. Zhang, T. Zhao, P. Duffy, Y. Dong, A.N. Annaidh, E. O'Cearbhaill, W. Wang, Hydrolytically degradable hyperbranched PEG-polyester adhesive with low swelling and robust mechanical properties, Adv Healthcare Mater. (2015) (n/a-n/a).
[11] M.A. Woodruff, D.W. Hutmacher, The return of a forgotten polymer—polycaprolactone in the 21st century, Prog. Polym. Sci. 35 (10) (2010) 1217–1256.
[12] H.S. Shirazi, P.K. Forooshani, B. Pingguan-Murphy, I. Djordjevic, Processing and characterization of elastomeric polycaprolactone triol–citrate coatings for biomedical applications, Prog. Org. Coating 77 (4) (2014) 821–829.
[13] S.M. Korneev, Valence isomerization between diazo compounds and diazirines, Eur. J. Org Chem. 31 (2011) 6153–6175.
[14] A.B. Kumar, J.D. Tipton, R. Manetsch, 3-Trifluoromethyl-3-aryldiazirine photolabels with enhanced ambient light stability, Chem. Commun. 52 (13) (2016) 2729–2732.
[15] O. Prucker, T. Brandstetter, J. Ruhe, Surface-attached hydrogel coatings via C,H-insertion crosslinking for biomedical and bioanalytical applications (Review), Biointerphases 13 (1) (2017), 010801.
[16] X.L. Peng, A. Migani, Q.S. Li, Z.S. Li, L. Blancafort, Theoretical study of non-Hammett vs. Hammett behaviour in the thermolysis and photolysis of arylchlorodiazirines, Phys. Chem. Chem. Phys. 20 (2) (2018) 1181–1188.
[17] J.R. Hill, A.A.B. Robertson, Fishing for drug targets: a focus on diazirine photoaffinity probe synthesis, J. Med. Chem. 61 (16) (2018) 6945–6963.
[18] M. Singh, C.S. Yin, S.J. Page, Y. Liu, G. Wicaksono, R. Pujar, S.K. Choudhary, G. U. Kulkarni, J. Chen, J.V. Hanna, R.D. Webster, T.W.J. Steele, Synergistic voltaglue adhesive mechanisms with alternating electric fields, Chem. Mater. 32 (6) (2020) 2440–2449.
[19] G. Feng, I. Djordjevic, V. Mogal, R. O'Rorke, O. Pokholenko, T.W. Steele, Elastic light tunable tissue adhesive dendrimers, Macromol. Biosci. 16 (7) (2016) 1072–1082.
[20] V. Mogal, V. Papper, A. Chaurasia, G. Feng, R. Marks, T. Steele, Novel on-demand bioadhesion to soft tissue in wet environments, Macromol. Biosci. 14 (4) (2014) 478–484.
[21] J. Ping, F. Gao, J.L. Chen, R.D. Webster, T.W.J. Steele, Adhesive curing through low-voltage activation, Nat. Commun. 6 (2015).
[22] A. Blencowe, C. Blencowe, K. Cosstick, W. Hayes, A carbene insertion approach to functionalised poly(ethylene oxide)-based gels, React. Funct. Polym. 68 (4) (2008) 868–875.
[23] A. Blencowe, W. Fagour, C. Blencowe, K. Cosstick, W. Hayes, Synthesis of hyperbranched poly(aryl amine)s via a carbene insertion approach, Org. Biomol. Chem. 6 (13) (2008) 2327–2333.
[24] A.K. Bertram, M.T.H. Liu, Cycloaddition of arylchlorocarbenes using ultrasound, J. Chem. Soc., Chem. Commun. (5) (1993) 467–468.
[25] C. Marionnet, C. Tricaud, F. Bernerd, Exposure to non-extreme solar UV daylight: spectral characterization, effects on skin and photoprotection, Int. J. Mol. Sci. 16 (1) (2015) 68–90.
[26] L.E. Corum, V. Hlady, Screening platelet–surface interactions using negative surface charge gradients, Biomaterials 31 (12) (2010) 3148–3155.
[27] M. Foox, M. Ben-Tzur, N. Koifman, M. Zilberman, Effect of gamma radiation on novel gelatin alginate–based bioadhesives, International Journal of Polymeric Materials and Polymeric Biomaterials 65 (12) (2016) 611–618.
[28] R. Bonneau, M.T.H. Liu, Quantum yield of formation of diazo compounds from the photolysis of diazirines, J. Am. Chem. Soc. 118 (30) (1996) 7229–7230.
[29] N. Kanoh, Photo-cross-linked small-molecule affinity matrix as a tool for target identification of bioactive small molecules, Nat. Prod. Rep. 33 (5) (2016) 709–718.
[30] Y. Zhang, L. Wang, R.A. Moss, M.S. Platz, Ultrafast spectroscopy of arylchlorodiazirines: hammett correlations of excited state lifetimes, J. Am. Chem. Soc. 131 (46) (2009) 16652–16653.
[31] S.I. Ivlev, A.J. Karttunen, M.R. Buchner, M. Conrad, R.V. Ostvald, F. Kraus, Synthesis and characterization of barium hexafluoridoosmates, Crystals 8 (1) (2018) 11.
[32] B. Musio, E. Gala, S.V. Ley, Real-time spectroscopic analysis enabling quantitative and safe consumption of fluoroform during nucleophilic trifluoromethylation in flow, ACS Sustain. Chem. Eng. 6 (1) (2018) 1489–1495.
[33] S.M. Korneev, Valence isomerization between diazo compounds and diazirines, Eur. J. Org Chem. 31 (2011) (2011) 6153–6175.
[34] J. Brunner, H. Senn, F.M. Richards, 3-Trifluoromethyl-3-phenyldiazirine. A new carbene generating group for photolabeling reagents, J. Biol. Chem. 255 (8) (1980) 3313–3318.
[35] M. Nassal, 4-(1-Azi-2, 2, 2-trifluoroethyl) benzoic acid, a highly photolabile carbene generating label readily fixable to biochemical agents, Liebigs Ann. Chem. 9 (1983) (1983) 1510–1523.
[36] P. The, International commission on non-ionizing radiation, guidelines ON limits OF exposure to ultraviolet radiation OF wavelengths between 180 nm and 400 nm (incoherent optical radiation), Health Phys. 87 (2) (2004).
[37] L. Dong-Xu, W. Hong-Ning, W. Chun-Ling, L. Hong, S. Ping, Y. Xiao, Modulus of elasticity of human periodontal ligament by optical measurement and numerical simulation, Angle Orthod. 81 (2) (2011) 229–236.
[38] N. Yoshida, Y. Koga, C.-L. Peng, E. Tanaka, K. Kobayashi, In vivo measurement of the elastic modulus of the human periodontal ligament, Med. Eng. Phys. 23 (8) (2001) 567–572.
[39] Y.N. Feng, Y.P. Li, C.L. Liu, Z.J. Zhang, Assessing the elastic properties of skeletal muscle and tendon using shearwave ultrasound elastography and MyotonPRO, Sci. Rep. 8 (1) (2018) 17064.
[40] P.V. Kolluru, J. Lipner, W. Liu, Y. Xia, S. Thomopoulos, G.M. Genin, I. Chasiotis, Strong and tough mineralized PLGA nanofibers for tendon-to-bone scaffolds, Acta Biomater. 9 (12) (2013) 9442–9450.
[41] X.-M. Shi, F.-M. Wu, B. Jing, N. Wang, L.-L. Xu, S.-F. Pang, Y.-H. Zhang, Hygroscopicity of internally mixed particles composed of (NH4) 2SO4 and citric acid under pulsed RH change, Chemosphere 188 (2017) 532–540.
[42] D. Gómez-Martínez, P. Partal, I. Martínez, C. Gallegos, Rheological behaviour and physical properties of controlled-release gluten-based bioplastics, Bioresour. Technol. 100 (5) (2009) 1828–1832.
[43] A.R. Ferreira, C.A. Torres, F. Freitas, M.A. Reis, V.D. Alves, I.M. Coelhoso, Biodegradable films produced from the bacterial polysaccharide FucoPol, Int. J. Biol. Macromol. 71 (2014) 111–116.
[44] J. Wang, J.A. Kaplan, Y.L. Colson, M.W. Grinstaff, Mechanoresponsive materials for drug delivery: harnessing forces for controlled release, Adv. Drug Deliv. Rev. 108 (2017) 68–82.
[45] D.F. Williams, On the mechanisms of biocompatibility, Biomaterials 29 (20) (2008) 2941–2953.
[46] S.N. Rodrigues, I.C. Gonçalves, M. Martins, M.A. Barbosa, B.D. Ratner, Fibrinogen adsorption, platelet adhesion and activation on mixed hydroxyl-/methyl-terminated self-assembled monolayers, Biomaterials 27 (31) (2006) 5357–5367.
[47] W. Okrój, M. Walkowiak-Przybyło, K. Rośniak-Bak, L. Klimek, B. Walkowiak, Comparison of microscopic methods for evaluating platelet adhesion to biomaterial surfaces, Acta Bioeng. Biomech. 11 (2) (2009) 45–49.
[48] J. Kim, K.-W. Lee, T.E. Hefferan, B.L. Currier, M.J. Yaszemski, L. Lu, Synthesis and evaluation of novel biodegradable hydrogels based on poly (ethylene glycol) and sebacic acid as tissue engineering scaffolds, Biomacromolecules 9 (1) (2007) 149–157.
[49] D. Motlagh, J. Yang, K.Y. Lui, A.R. Webb, G.A. Ameer, Hemocompatibility evaluation of poly(glycerol-sebacate) in vitro for vascular tissue engineering, Biomaterials 27 (24) (2006) 4315–4324.
[50] H.S. Nanda, A.H. Shah, G. Wicaksono, O. Pokholenko, F. Gao, I. Djordjevic, T.W. J. Steele, Nonthrombogenic hydrogel coatings with carbene-cross-linking bioadhesives, Biomacromolecules 19 (5) (2018) 1425–1434.
[51] L. Dubinsky, B.P. Krom, M.M. Meijler, Diazirine based photoaffinity labeling, Bioorg. Med. Chem. 20 (2) (2012) 554–570.
[52] X. Wang, X. Wang, J. Wang, Application of carbene chemistry in the synthesis of organofluorine compounds, Tetrahedron 75 (8) (2019) 949–964.
[53] S. Kempe, K. Mäder, In situ forming implants — an attractive formulation principle for parenteral depot formulations, J. Contr. Release 161 (2) (2012) 668–679.
[54] A.L. Balocco, P.G.E. Van Zundert, S.S. Gan, T.J. Gan, A. Hadzic, Extended release bupivacaine formulations for postoperative analgesia: an update, Curr.t Opin. Anesthesiol. 31 (5) (2018) 636–642.
[55] D.C. Richard, Medical Toxicology, third ed., Lippincott, Williams & Wilkins, Philadelphia, 2004, p. 1232, 2004.
[56] V. Velanovich, P. Rider, K. Deck, H.S. Minkowitz, D. Leiman, N. Jones, G. Niebler, Safety and efficacy of bupivacaine HCl collagen-matrix implant (INL-001) in open inguinal hernia repair: results from two randomized controlled trials, Adv. Ther. 36 (1) (2019) 200–216.
[57] D. Hu, E. Onel, N. Singla, W.G. Kramer, A. Hadzic, Pharmacokinetic profile of liposome bupivacaine injection following a single administration at the surgical site, Clin. Drug Invest. 33 (2) (2013) 109–115.
[58] S.R. Chung, M.M. Choudhury, S.J.Y. Too, C.B. Ong, T.W.J. Steele, D. A. McGrouther, A.Y.H. Chin, Microvascular anastomosis with fish-mouth suturing and adhesive sealants, J. Plast. Reconstr. Aesthetic Surg. : JPRAS 72 (1) (2019) 137–171.
[59] Q. Pellenc, J. Touma, R. Coscas, G. Edorh, M. Pereira, J. Karp, Y. Castier, P. Desgranges, J. Alsac, Preclinical and clinical evaluation of a novel synthetic bioresorbable, on demand light activated sealant in vascular reconstruction, J. Cardiovasc. Surg. (2019).
[60] E.M. Sussman, M.C. Halpin, J. Muster, R.T. Moon, B.D. Ratner, Porous implants modulate healing and induce shifts in local macrophage polarization in the foreign body reaction, Ann. Biomed. Eng. 42 (7) (2014) 1508–1516.
[61] A. Narayanan, S. Kaur, C. Peng, D. Debnath, K. Mishra, Q. Liu, A. Dhinojwala, A. Joy, Viscosity attunes the adhesion of bioinspired low modulus polyester adhesive sealants to wet tissues, Biomacromolecules 20 (7) (2019) 2577–2586.
[62] H. Takeuchi, H. Kishioka, K. Kitajima, Efficient and/or selective methylation by diazomethane of alcohols, halo alcohols, glycols, amino alcohols and mercapto alcohols with the use of a proton-exchanged X-type zeolite as an acid–base bifunctional catalyst, J. Phys. Org. Chem. 8 (2) (1995) 121–126.
[63] N. Kanoh, T. Nakamura, K. Honda, H. Yamakoshi, Y. Iwabuchi, H. Osada, Distribution of photo-cross-linked products from 3-aryl-3-trifluoromethyldiazirines and alcohols, Tetrahedron 64 (24) (2008) 5692–5698.
[64] K.A. Mix, R.T. Raines, Optimized diazo scaffold for protein esterification, Org. Lett. 17 (10) (2015) 2358–2361.
[65] A. Blencowe, N. Caiulo, K. Cosstick, W. Fagour, P. Heath, W. Hayes, Synthesis of hyperbranched poly (aryl ether) s via carbene insertion processes, Macromolecules 40 (4) (2007) 939–949.
[66] S.A. Fleming, Chemical reagents in photoaffinity labeling, Tetrahedron 51 (46) (1995) 12479–12520.

[67] J. Guo, W. Wang, J. Hu, D. Xie, E. Gerhard, M. Nisic, D. Shan, G. Qian, S. Zheng, J. Yang, Synthesis and characterization of anti-bacterial and anti-fungal citrate-based mussel-inspired bioadhesives, Biomaterials 85 (2016) 204–217.
[68] G.P. Sailema-Palate, A. Vidaurre, A.J. Campillo-Fernández, I. Castilla-Cortázar, A comparative study on Poly(ε-caprolactone) film degradation at extreme pH values, Polym. Degrad. Stabil. 130 (2016) 118–125.
[69] C.X. Lam, M.M. Savalani, S.H. Teoh, D.W. Hutmacher, Dynamics of in vitro polymer degradation of polycaprolactone-based scaffolds: accelerated versus simulated physiological conditions, Biomed. Mater. 3 (3) (2008), 034108.
[70] N. Elimelech, Dotan, Ana, Ophir, Amos, Bioadhesive Composition and Device for Repairing Tissue Damage, MEDIZN TECHNOLOGIES LTD., United States, 2011.
[71] P. Ferreira, J.F.J. Coelho, M.H. Gil, Development of a new photocrosslinkable biodegradable bioadhesive, Int. J. Pharm. 352 (1) (2008) 172–181.
[72] A. Shagan, W. Zhang, M. Mehta, S. Levi, D.S. Kohane, B. Mizrahi, Hot glue gun releasing biocompatible tissue adhesive, Adv. Funct. Mater. 0(0) 1900998.
[73] A. Shagan, T. Croitoru-Sadger, E. Corem-Salkmon, B. Mizrahi, Near-infrared light induced phase transition of biodegradable composites for on-demand healing and drug release, ACS Appl. Mater. Interfaces 10 (4) (2018) 4131–4139.
[74] D.S. Marques, J.M.C. Santos, P. Ferreira, T.R. Correia, I.J. Correia, M.H. Gil, C.M.S. G. Baptista, Photocurable bioadhesive based on lactic acid, Mater. Sci. Eng. C 58 (2016) 601–609.
[75] M. Pereira, Brillaud, Elsa, Sealant Composition, GECO BIOMEDICAL, France, 2016.
[76] N. Fujii, H. Uchida, T. Saito, The damaging effect of UV-C irradiation on lens alpha-crystallin, Mol. Vis. 10 (2004) 814–820.
[77] N. Annabi, Y.N. Zhang, A. Assmann, E.S. Sani, G. Cheng, A.D. Lassaletta, A. Vegh, B. Dehghani, G.U. Ruiz-Esparza, X. Wang, S. Gangadharan, A.S. Weiss, A. Khademhosseini, Engineering a highly elastic human protein-based sealant for surgical applications, Sci. Transl. Med. 9 (410) (2017).
[78] F. Liu, Z. Wang, C. Lü, L. Gao, M. Ding, Gamma ray irradiation-initiated copolymerization of a binary casting system involving DPBMIn and vinylpyrrolidone, Macromol. Mater. Eng. 290 (7) (2005) 726–732.
[79] F. Hosni, K. Farah, H. Kaouach, A. Louati, R. Chtourou, A.H. Hamzaoui, Effect of gamma-irradiation on the colorimetric properties of epoxy-resin films: potential use in dosimetric application, Nucl. Instrum. Methods Phys. Res. Sect. B Beam Interact. Mater. Atoms 311 (2013) 1–4.
[80] L. Gan, N.C. Tan, A.H. Shah, R.D. Webster, S.L. Gan, T.W. Steele, Voltage-activated adhesion through donor–acceptor dendrimers, Macromolecules 51 (17) (2018) 6661–6672.
[81] J. Ping, F. Gao, J.L. Chen, R.D. Webster, T.W. Steele, Adhesive curing through low-voltage activation, Nat. Commun. 6 (2015) 8050.
[82] H.U. Zaman, M. Beg, Improvement of physico-mechanical, thermomechanical, thermal and degradation properties of PCL/gelatin biocomposites: effect of gamma radiation, Radiat. Phys. Chem. 109 (2015) 73–82.
[83] R. Michel, L. Poirier, Q. van Poelvoorde, J. Legagneux, M. Manassero, L. Corté, Interfacial fluid transport is a key to hydrogel bioadhesion, Proc. Natl. Acad. Sci. Unit. States Am. 116 (3) (2019) 738–743.